Technical University of Denmark

DTU

Simulations of super-structure domain walls in two dimensional assemblies of magnetic nanoparticles

Jordanovic, Jelena; Beleggia, Marco; Schiøtz, Jakob; Frandsen, Cathrine

[Link back to DTU Orbit](#)

DTU Library
Technical Information Center of Denmark

Simulations of super-structure domain walls in two dimensional assemblies of magnetic nanoparticles

J. Jordanovic, M. Beleggia, J. Schiøtz, and C. Frandsen

Articles you may be interested in

Self-assembled magnetic nanospheres with three-dimensional magnetic vortex
Appl. Phys. Lett. **105**, 232402 (2014); 10.1063/1.4903741

Correlation between magnetism and electronic structure of Zn1−xCoxO nanoparticles
J. Appl. Phys. **113**, 17C302 (2013); 10.1063/1.4794355

Role of oxygen defects on the magnetic properties of ultra-small Sn1−xFexO2 nanoparticles
J. Appl. Phys. **113**, 17B504 (2013); 10.1063/1.4794140

Entropy change linked to the magnetic field induced Morin transition in Hematite nanoparticles
Appl. Phys. Lett. **100**, 063102 (2012); 10.1063/1.3682084

Direct visualization of dipolar ferromagnetic domain structures in Co nanoparticle monolayers by electron holography
Appl. Phys. Lett. **93**, 082502 (2008); 10.1063/1.2973675

Simulations of super-structure domain walls in two dimensional assemblies of magnetic nanoparticles

J. Jordanovic,[1] M. Beleggia,[2,3] J. Schiøtz,[1,4] and C. Frandsen[1]

[1]*Department of Physics, Technical University of Denmark, DK-2800 Kgs. Lyngby, Denmark*
[2]*Center for Electron Nanoscopy (CEN), Technical University of Denmark, DK-2800 Kgs. Lyngby, Denmark*
[3]*Helmholtz-Zentrum-Berlin für Materialen und Energie, Hahn-Meitner-Platz 1, 14109 Berlin, Germany*
[4]*DNRF Center for Individual Nanoparticle Functionality (CINF), Technical University of Denmark, DK-2800 Kgs. Lyngby, Denmark*

We simulate the formation of domain walls in two-dimensional assemblies of magnetic nanoparticles. Particle parameters are chosen to match recent electron holography and Lorentz microscopy studies of almost monodisperse cobalt nanoparticles assembled into regular, elongated lattices. As the particles are small enough to consist of a single magnetic domain each, their magnetic interactions can be described by a spin model in which each particle is assigned a macroscopic "superspin." Thus, the magnetic behaviour of these lattices may be compared to magnetic crystals with nanoparticle superspins taking the role of the atomic spins. The coupling is, however, different. The superspins interact only by dipolar interactions as exchange coupling between individual nanoparticles may be neglected due to interparticle spacing. We observe that it is energetically favorable to introduce domain walls oriented along the long dimension of nanoparticle assemblies rather than along the short dimension. This is unlike what is typically observed in continuous magnetic materials, where the exchange interaction introduces an energetic cost proportional to the area of the domain walls. Structural disorder, which will always be present in realistic assemblies, pins longitudinal domain walls when the external field is reversed, and makes a gradual reversal of the magnetization by migration of longitudinal domain walls possible, in agreement with previous experimental results. © 2015 AIP Publishing LLC. [http://dx.doi.org/10.1063/1.4926730]

I. INTRODUCTION

Magnetic nanoparticles have potential as building blocks to fabricate materials and devices as, for example, sensors,[1] storage media,[2] and permanent magnets,[3–5] with new magnetic properties that are not present in bulk (continuous) magnets. The anisotropic magnetostatic interaction between the magnetic moments of the particles can be the driving mechanism for self-assembly into chains[6,7] and dendrite-like shapes,[8] leading to complex pattern formation. In combination with the application of different nanofabrication techniques,[9] it is possible to achieve columnar structures, closed-packed grids, and thin film aggregates.[10,11] Methods for creating these low-dimensional structures are, for example, polymer-mediated[12] or dry-mediated[13] fabrication techniques.

When single-domain magnetic particles form lattice structures, there is the possibility that magnetic interactions leads to magnetic ordering of the nanoparticle moments. Dipolar ferromagnetic ordering was first predicted by Luttinger and Tisza[14] in 1946 for an fcc lattice of point dipoles. Such magnetic ordering is sometimes referred to as "superferromagnetic" to indicate that it is referring to magnetic ordering in the "superlattice" of nanoparticles, and not the magnetic ordering of the atoms in the nanoparticles itself. Hence, there is the possibility to introduce different superdomains, and thus domain walls in the superlattice. In the absence of exchange coupling between the particles, there is no reason for the domain walls to have finite width, and sharp

walls may form between adjacent rows of nanoparticles. In the following discussion, we shall omit the prefix "super-," as there is no risk of confusion between the nanoparticle structures and atomic structures.

Magnetic nanoparticle structures have been analyzed theoretically over the years. Scheinfein *et al.*[15] study very small (a few nanometer sized) iron islands and observe ferromagnetic ordering for particles with a diameter around 3 nm. They find that Monte Carlo simulations can only reproduce this if direct exchange coupling between neighboring particles is included, probably because the dipolar interaction is too weak. Assemblies of larger particles show ferromagnetic order without exchange coupling.[14,16–19] Several papers notice that while an infinite hexagonal lattice of magnetic dipoles displays ferromagnetic ordering, finite systems can lower their energy by forming often complex vortex structures.[20,21] Vedmedenko *et al.*[22] review these simulations, but their main focus is on the contribution from higher multipole moments, which can be considered absent in case of spherical particles. With the advent of advanced electron microscopy methods, such as electron holography, a direct visualization of the magnetic ordering became available to experimental analysis tools (see, e.g., Ref. 23), which refreshes our view on magnetic order and domain wall formation.

We recently discussed[24] Lorenz microscopy and electron holography studies of elongated rope-like assemblies of cobalt nanoparticles which displayed the affinity to develop long domain walls along the ropes. This feature differs from

conventional continuous magnetic materials, where domain walls often try to be as short as possible. Moreover, we observed using Lorentz microscopy that longitudinal walls also form when an external field is applied, and that domain walls sweep in transversal direction of the structures in presence of a magnetic field. We supported the observations with a simulation analysis, indicating that structural disorder may support long domain walls and enhance the possibilities of the domain sweeping.

In this paper, we report extensive simulations of two-dimensional assemblies of magnetic nanoparticles, and discuss the role of the structural arrangement of the nanoparticles and how this influences the domain structure, with the aim of being able to control the magnetic structure by controlling the layout of the nanoparticles. We focus, in particular, on three classes of domain structure, which we call the "ferromagnetic state" (the F-state), the "longitudinal domain wall" (the L-state), and the "transversal domain wall" (the T-state), see Figure 1.

II. METHODS

We model assemblies of a monolayer of identical nanoparticles, either placed on a regular, hexagonal lattice, or perturbed from the regular positions, but in all cases, the nanoparticles are kept stationary. Each nanoparticle has a magnetic moment which is free to rotate, and they interact through the dipolar magnetic interactions. In addition, an external magnetic field may be applied. Free boundary conditions are applied to the system. The energy of the system is thus given by

$$U = \frac{\mu_0}{4\pi} \sum_{i,j \neq i} \left(\frac{\vec{\mu}_i \cdot \vec{\mu}_j}{r_{ij}^3} - 3 \frac{(\vec{\mu}_i \cdot \vec{r}_{ij})(\vec{\mu}_j \cdot \vec{r}_{ij})}{r_{ij}^5} \right) - \sum_i \vec{\mu}_i \cdot \vec{B}_{\text{ext}}, \tag{1}$$

where μ_0 is the vacuum permeability, $\vec{\mu}_i$ is the magnetic moment of particle i, $\vec{r}_{ij}$ is the center-to-center distance vector between particle i and j, and $\vec{B}_{\text{ext}}$ is the applied magnetic field. In these simulations, all magnetic moments have the same magnitude, μ, and we define the dipole interaction parameter

$$\epsilon = \frac{\mu_0 \mu^2}{4\pi d^3}, \tag{2}$$

where d is the nearest-neighbor distance in the hexagonal lattice.

We do not include a term describing magnetic anisotropy in Eq. (1). Two different limits correspond to omitting this term, the most obvious being the limit of vanishing anisotropy. The opposite limit, that of infinite anisotropy in connection with freely rotating particles, results in the same energy expression with the magnetic moment locked along the easy axis.

To investigate the energetics of the nanoparticle assemblies, we perform thermostated molecular dynamics simulations (MD) at a low temperature. In the MD simulations, particles are allowed to rotate but not to move. This corresponds to a system of particles loosely bound to a substrate, e.g., as occurring during the final phase of evaporation-mediated assembly.

We chose an MD approach over solving the full Landau-Lifshitz-Gilbert (LLG) equations, as the LLG equation leads to a separation of time scales between the fast dynamics of the magnetic moments and the slow dynamics of the nanoparticles. The particles thus to good approximation only see the final equilibrium of the magnetic moments and are unaffected by the rapid precessional motion leading to it; in particular, there are no rapid fluctuations in the fields to excite the magnetic degrees of freedom. This is equivalent with the prevalent use of the Born-Oppenheimer approximation in atomic-scale simulations.

The equations of motion of rotating particles with rotational symmetry along an axis (the axis of the magnetic moment) can conveniently be written as[25]

$$\frac{\partial}{\partial t} \vec{e}_i = \vec{u}_i, \tag{3}$$

$$\frac{\partial}{\partial t} \vec{u}_i = \frac{1}{I} \vec{g}_i + \lambda_i \vec{e}_i, \tag{4}$$

where $\vec{e}_i$ is a unit vector along the axis of symmetry of particle i ($\vec{\mu}_i = \mu \vec{e}_i$), $\vec{u}_i$ is its time derivate, and I is the moment of inertia, which is a scalar as the particles are spherical. $\vec{g}_i$ is related to the torque $\vec{\tau}$ on the particle by $\vec{\tau}_i = \vec{e}_i \times \vec{g}_i$ and the requirement that $\vec{g}_i$ and $\vec{e}_i$ are perpendicular, and can be calculated from the energy by

$$\vec{g}_i = \vec{f}_i - \left(\vec{f}_i \cdot \vec{e}_i \right) \vec{e}_i; \quad \vec{f}_i = \frac{\partial U}{\partial \vec{e}_i}. \tag{5}$$

The Lagrange multiplier λ_i ensures that $\vec{e}_i$ remains a unit vector. The equations of motion can now be integrated using the leap-frog algorithm coupled with a Berendsen thermostat[26] following the algorithm described by Allen and Tildesley[25]
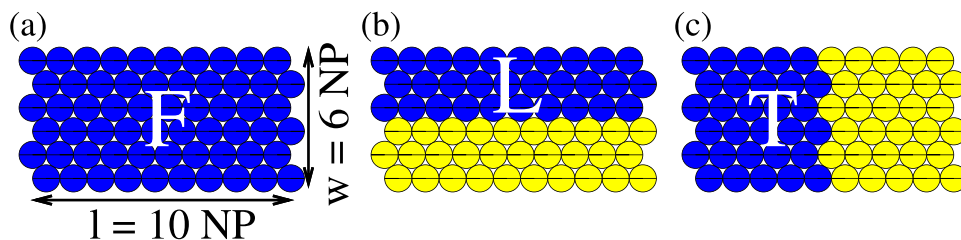
FIG. 1. The three main types of magnetic domain ordering in elongated structures of closed-packed nanoparticles. (a) The ferromagnetic state (called the F-state) with all magnetic moments aligned along the long direction of the assembly. (b) The state with a longitudinal domain wall (L-state). (c) The state with a transversal domain wall (T-state). In all cases, blue particles signify a magnetic moment pointing to the right, yellow a magnetic moment pointing to the left.

$$\lambda_i = -\frac{2}{\delta t}\vec{u}_i\left(t - \frac{1}{2}\delta t\right)\cdot\vec{e}_i(t), \tag{6}$$

$$\chi = \sqrt{1 + \frac{\delta t}{\tau_{\text{rel}}}\left(\frac{T}{T(t)} - 1\right)}, \tag{7}$$

$$\vec{u}_i\left(t + \frac{1}{2}\delta t\right) = (2\chi - 1)\vec{u}_i\left(t - \frac{1}{2}\delta t\right)$$
$$+ \chi\left(\frac{1}{I}\vec{g}_i(t) + \lambda_i\vec{e}_i(t)\right)\delta t, \tag{8}$$

$$\vec{e}_i(t + \delta t) = \vec{e}_i(t) + \vec{u}_i\left(t + \frac{1}{2}\delta t\right)\delta t, \tag{9}$$

where T is the desired temperature, $T(t)$ is the instantaneous temperature calculated from the kinetic energy, and τ_{rel} is a relaxation time for the temperature equilibration.

We have chosen to perform molecular dynamics at low temperature instead of a simple energy minimization, as it gives a physical meaningful path between the starting configuration and the final configuration, and allow us to later include the motion of the particles.[27]

We use values for μ and for the moment of inertia I of the nanoparticles corresponding to a type of cobalt nanoparticles (NPs) as used by Varón et al.[24] The particles have diameter of $\sigma = 15\,\text{nm}$, and magnetic saturation $M_s = 1.4 \times 10^6\,\text{A/m}$, which leads to a magnetic moment of $\mu = 2.47 \times 10^{-18}\,\text{Am}^2$. The density of cobalt is $\rho = 8.9 \times 10^3\,\text{kg/m}^3$, leading to a moment of inertia of $I = 3.54 \times 10^{-37}\,\text{kg m}^2$. We chose a grid spacing equal to the particle diameter, giving a dipole interaction parameter $\epsilon = 1.8 \times 10^{-19}\,\text{J}$, corresponding to a characteristic temperature of $1.3 \times 10^4\,\text{K}$.

Our simulations ignore the magnetic anisotropy of the nanoparticles. Typically, the main contribution to the magnetic anisotropy of nanoparticles comes from a non-spherical shape rather than from the crystalline anisotropy.[28,29] The magnetic anisotropy energy of cubic Co (the ϵ phase usually found in nanoparticles) is around $5 \times 10^4\,\text{J/m}^3$ (Ref. [28]), giving a magnetic anisotropy energy of $10^{-19}\,\text{J}$. However, in the case of freely rotating nanoparticles, the anisotropy becomes irrelevant for the final configurations and will only influence the path taken toward the minimum energy configuration, and the time needed to reach the minimum.

In our simulations, we use open boundary conditions, so that we can observe edge effects. As starting conditions, we set angular momenta to zero and all magnetic moment orientations starting in-plane of the grid. Although we only model two-dimensional nanoparticle assemblies, the magnetic moments are free to rotate in all three dimensions. However, as precession is not inherent to these equations, the magnetic moments will not deviate out of the plane during the simulation, unless they initially are out of plane or an external magnetic field is applied out of plane.

III. RESULTS AND DISCUSSION

A. Longitudinal and transverse domain walls in regular structures

After introducing the three different magnetic configurations, the F-, L-, and T-states (see Fig. 1), we first discuss the

static, non-equilibrated properties of the configurations, before performing MD simulations. We focus on the energy difference between the states. Therefore, we compare the dipole-dipole interaction energies for a range of lengths $l = 2, 4, 6, \ldots, 140$ NP and widths $w = 2, 4, \ldots, 20$ NP of the assemblies. For visualization purposes, we plot the unit-less energy difference per atom, $\Delta U/(\epsilon N)$, where ΔU is the difference in the interaction energy given in Eq. (1) with no external field ($\vec{B}_{\text{ext}} = 0$). The comparison is shown in Fig. 2.

We determine the preferred state by comparing the energies. We find that the T-state is never the lowest in energy, and is therefore not favored. The competition between the one-domain F-state and the longitudinal domain wall appears to be decided by the aspect ratio l/w of the nanoparticle assembly. For long assemblies, $l/w > 4$, the F-state dominates, whereas wider assemblies prefer the state with a longitudinal domain wall. This is in stark contrast to continuous magnetic materials, where there is a significant cost in exchange energy to introduce a domain wall, leading to the transversal domain walls being favored, simply because they minimize the area of the domain wall. As the inter-particle exchange contribution to the energy is absent, it is only the magnetic dipole interaction that controls the energetics.

Adding an external field perturbs this result, as it either increases or decreases the energy of the fully magnetized F-state, whereas the energy of the L state is unchanged. The favored state is then no longer just determined by the aspect ratio and the dividing line between the two phases curves.

The appearance of the longitudinal domain wall has its roots in the highly anisotropic interaction of the magnetic
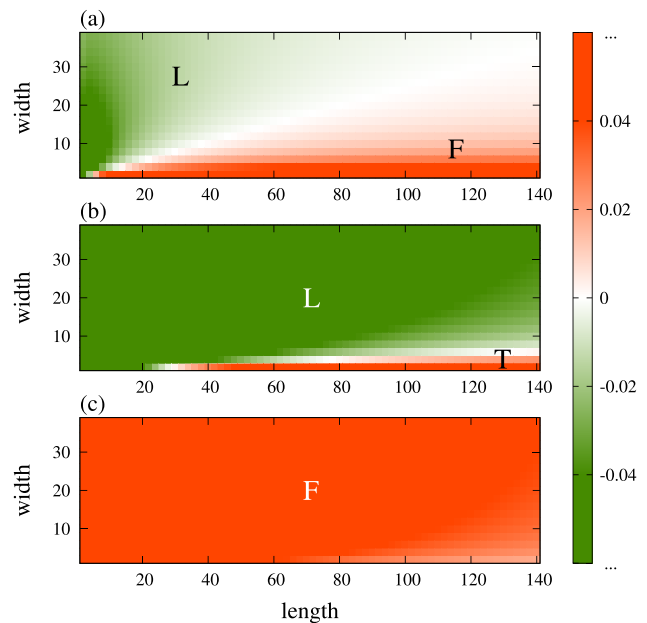

FIG. 2. Phase diagram of the unit less energy difference per particle between (a) L- and F-states, (b) L- and T-states, and (c) F- and T-states. The color shows the energy difference between the two states, for example, in the upper panel, the green color signifies that $E_L - E_F < 0$, meaning that the L-state is energetically favoured. In parts of the phase diagram, the color scale is allowed to saturate. We see how the T-state is always unfavorable with respect to the F-state. Thus, the complete phase diagram is identical to the upper panel. For very long, needle-like structures, the ferromagnetic F-state is favored, whereas wider structures favor the longitudinal domain wall.
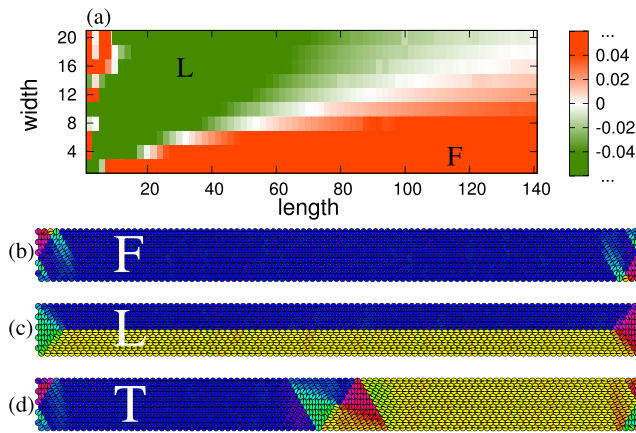
FIG. 3. The three magnetic states and their relative stability after relaxation of the magnetic structure. (a) The F-state remains the most stable state for very long structures, while the L-state is preferred for wider structures, but relaxation moves the boundary between the two regimes toward higher aspect ratios. For very wide systems (aspect ratios below 2:1), the original magnetic structure is lost, see text and Fig. 4. (b)–(d) Typical magnetic structure for the three phases, here shown for a system of length 100 and width 10. Panel (a) is adapted from Ref. 24.

dipoles. In a long chain of magnetic dipoles, there is a strong ferromagnetic coupling between the dipoles. However, adjacent chains may couple either ferromagnetically or antiferromagnetically. Varón *et al.*[30] have calculated the magnetic field of a long, perfectly oriented chain of dipoles, showing that adjacent chains couple ferromagnetically if they are closed packed, but antiferromagnetically in a square packing. Although neighboring chains couple ferromagnetically in a closed-packed hexagonal structure, the coupling between more remote chains will be antiferromagnetic. Thus, for a wide strip, the chains in the two sides (top and bottom row of nanoparticles in Fig. 1) would prefer to be antiferromagnetically coupled, and it is reasonable that it becomes favorable to introduce a longitudinal domain wall even though it causes the two neighboring chains across the wall to have unfavorable coupling. A transverse domain wall would, however, break the strong ferromagnetic coupling within all the chains.

So far, we have not allowed the magnetic moments of the nanoparticles to respond to the dipolar field of the other

particles. The molecular dynamics simulations allow the particles to rotate, and thus minimize the energy of the various structures. This changes the results quantitatively but not qualitatively. The new phase diagram and the corresponding magnetic structures are shown in Fig. 3. For most shapes, the initial magnetic state is still recognizable in the final state, as is seen in Figs. 3(b)–3(d). In systems with a low aspect ratio, $l/w < 2$, the magnetic state changes significantly and always to a more complicated domain structure. We never see a system developed from one of the three states to another.

For the more elongated systems, the F-state shows the smallest magnetic relaxation, where some moments near the ends rotate (Fig. 3(b)). The L-state forms two new triangular domains at the ends, closing the flux within the assembly. This gives a significant reduction in the energy of this state, and favors the L-state in a region where the F-state was previously favorable. The T-state shows the most dramatic reconfiguration, this is a symptom of the high energy of the transversal domain wall, where neighboring nanoparticles along the chains have their most unfavorable heads-on configuration. The energy is in this case lowered by forming a vortex structure at the domain wall. Despite this significant relaxation, the T-states remain energetically unfavorable.

In the relaxed systems, we still see the same two phases as in the unrelaxed systems. The L-state is favored for wider structures, whereas the F-state is favored for the longer ones, but due to the relaxations in the L-state, the boundary has moved to a higher aspect ratio, and is no longer purely determined by the aspect ratio, see Fig. 3(a). For the larger structures, the boundary is at approximately an aspect ratio of 7:1.

For aspect ratios smaller than 2:1, the original magnetic structure is lost during the simulation, and more complex magnetic structures appear, see Fig. 4. In these cases, the color on the phase diagram in Fig. 3(a) has little informative value, as it indicates if the L-state or F-state develops into the lowest energy complex state, but this final state often has little resemblance to the original state. The domain structures are often complex, with multiple vortices, similar to what has previously been seen in simulations of disk-shaped samples of spins on a similar hexagonal lattice.[20,21] Similar multi-domain formations are also known from continuous
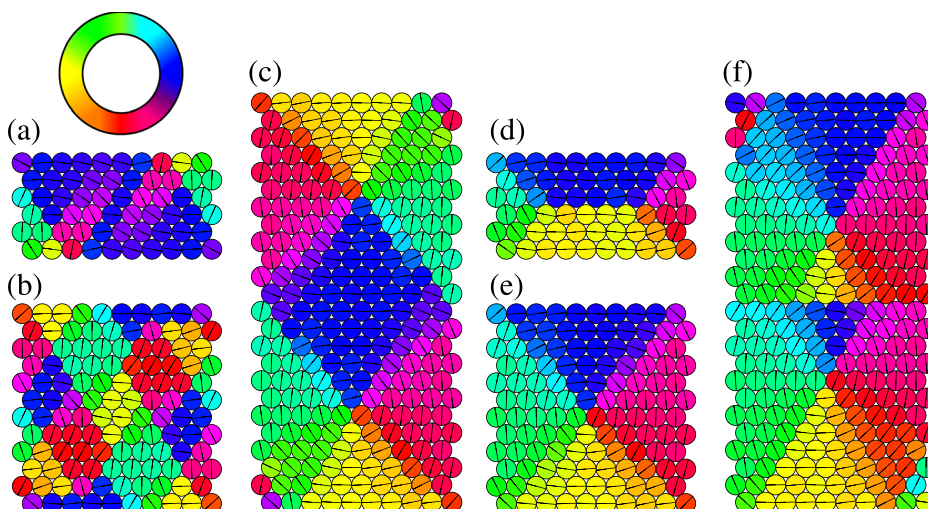

FIG. 4. Complex magnetic structures form when the aspect ratio is below 2:1. Starting from a ferromagnetic state, the F-state is still recognizable when the aspect ratio is 2:1 (a), but for aspect ratios of 1:1 (b) and 1:2 (c), the domain has broken up into multiple small domains. When starting from a longitudinal domain wall, the structure is maintained for both the 2:1(d) and 1:1 (c) aspect ratios, but in the latter case, it is no longer reasonable to call it a "longitudinal domain wall." For aspect ratios significantly below 1, multiple small domains again appear (f).

materials. In order to illustrate this, Fig. 4(c) shows a vortex–anti-vortex formation, whereas Fig. 4(f) shows two identical vortices separated by a cross-tie formation.[31]

B. Influence on structural disorder on the longitudinal domain wall

Since the magnetic coupling between adjacent chains of nanoparticles is only ferromagnetic at very short distances,[30] we would expect that increasing the distance between chains favors the L-state over the F-state. Figure 5 indeed shows that this is the case. When the distance between adjacent chains is increased by 10%, the critical aspect ratio increased from 4.1:1 to almost 14:1 for the unrelaxed structures. This trend continues for larger inter-chain distances, and slightly above a 25% increase, the ferromagnetic phase is no longer favourable for any aspect ratio. Presumably, the lowest energy configuration then becomes an antiferromagnetic state, but investigating this is outside the scope of this work.

In experimentally realisable structures, a certain amount of disorder is expected due to slight variation in nanoparticle size and geometry, and due to random processes during self-assembly. We model this by the introduction of a slight structural disorder. In order to model the disordered assemblies, we start with the moments placed on the hexagonal grid (with grid size equal to the particles' diameter $\sigma = 15\,\mathrm{nm}$) and change the position of each magnetic moment by a random vector created from a Gaussian distribution with a standard deviation of $\sigma_G = 0.1\sigma$. Without relaxing the magnetic moment, this leads to a smear-out of the boundary between the region favoring the L- and F-states, but disorder does not seem to systematically favor one state over the other.

After the MD runs, we see that the structural disorder induces a local magnetic disorder. Example snapshots of the relaxed disordered structures are shown in Figs. 6(b)–6(d). The magnetization pattern still resemble the initial states: in the relaxed disordered F-state (Fig. 6(b)), we see that the original magnetization still dominates; in the L-state (Fig. 6(c)), the longitudinal domain is still visible; and in the T-state (Fig. 6(d)), the transversal wall is smeared out, but still dividing the structure into two domains. The presented examples were typical for aspect ratios larger than two. Since the disorder does not change the overall dimensions of

FIG. 6. The role of disorder on the preferred domain structure. In (a), we see that disorder creates a region around aspect ratio 7:1 where the preferred magnetic state depends on the details of the nanoparticle configuration. (b)–(d) show that the magnetic state remains recognizable even in the presence of disorder. Panel (a) is adapted from Ref. 24.

the systems, the demagnetization fields can be assumed of the same order as in the non-disturbed case, leading to comparable reorganization of the moments at the edges.

The overall phase diagram (Fig. 6(a)) is relatively unperturbed by the disorder. Overall, we find the same states favored at the same aspect ratios as for the perfectly order systems, but the disorder smears out the transition between the F- and L-states, meaning that for aspect ratios near the critical value individual samples may behave in different ways depending on the details of the positions of the nanoparticles. The overall behaviour is, however, unchanged by the disorder, although as we shall see in Section III C, it helps pinning the domain walls when an external field is applied.

C. The role of disorder in an external magnetic field

Lorentz microscopy and electron holography[24] have previously shown that when a longitudinal wall is present, then a reversed field may move the wall in transversal direction. We were also able to show via simulations that disorder in the particle assembly is important to see this effect.[24] We here investigate if disorder may be important for inducing a longitudinal domain wall in a relaxed F-state. We analyzed ordered and disordered strips of the relaxed F-state, with length $l = 60$, and different widths, and subjected them to a magnetic field pointing opposite to the ferromagnetic order. The widths belong to either the F- or the L-regions, in both phase diagrams (Figs. 3 and 6). We increase the field in 0.5 mT steps, and allow the structure to relax (for about 50 000 time steps) at each step.

In Fig. 7, we monitored the normalized moment in the direction of the field as a function of the field strength. As the moment is normalized by the saturation magnetisation of the structure, the values of the plot lie between 1 and -1, where 1 is the original F-state, and, -1 the fully reversed F-state. An L-state would have a total magnetic moment of 0.

For the ordered structures (Fig. 7(a)), all curves show a shoulder towards values around 0.9 at low applied field strength, indicating that moments begin to turn. When we
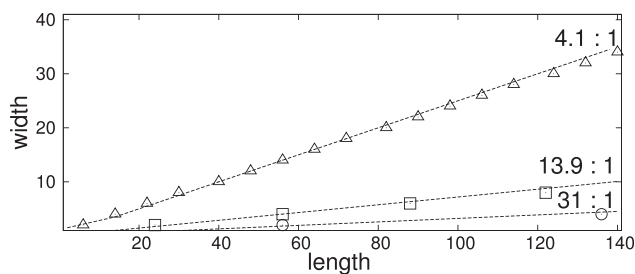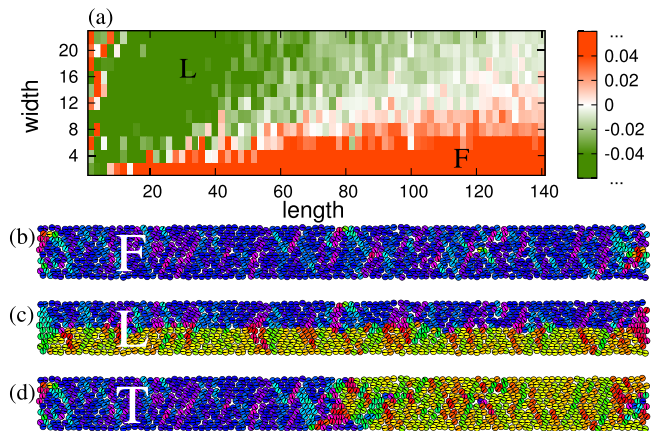

FIG. 5. When the distance between adjacent chains is increased, the ferromagnetic phase becomes less favourable. The three lines show the line separating the regions where the L- and F-states are most stable. Triangles: The fully closed-packed structure. Squares and circles: Structures with inter-chain distance increased by 10% and 25%, respectively. Since the dividing lines are straight, they correspond to a specific aspect ratio, which is written next to the lines.
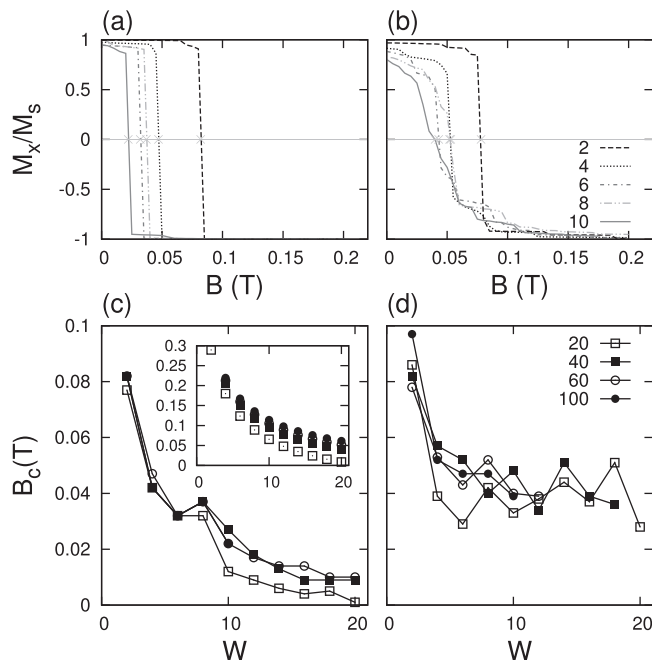
FIG. 7. Magnetic moment in direction of the field (M_x) as a function of the applied field strength B_{ext} for ordered (a) and disordered (b) systems. The legend indicates the width of the systems, in all cases, the length is 60. The corresponding coercive fields (B_c), defined as the field where $M_x = 0$, are shown as a function of the width (c) and (d), in this case, the legend indicates the lengths of the systems. The inset in (c) is a simple Stoner-Wohlfarth model of a continuous system switching as a whole, the same quantitative behaviour is seen, but at larger fields.

increase the field further, this leads to a sudden drop to values close to -1, indicating that all the moments are reversed. The threshold field value, at which the flip happens, moves to smaller values for wider strips. This effect is caused by the demagnetisation field of the nanoparticle assemblies.

We estimated the coercive field, by linearly interpolating the applied field value for zero moment. The result for a range of structures, with lengths, $l = 20, 40, 60,$ and 100, is plotted as function of the width, Fig. 7(c). We see that the coercive field (B_c) is almost determined by the width alone, and that the aspect ratio has a much smaller influence, in particular, in the case of low width/high aspect ratio. In the inset, we show a simple Stoner-Wohlfarth model,[32]

assuming a homogeneous single-domain system of the same size that is switching by rotation of the magnetization vector. Qualitatively, we see the same trend, although the absolute fields' strength is lower for the nanoparticles. This reflects that the system does not reverse homogeneously, but that a reversal nucleates at the ends and sweeps through the system, as discussed later. We interpret the similarity between the simulations and the Stoner-Wohlfarth model as an indication that it is in both cases the demagnetization factor that controls when the reversal sets in, although the mechanism of the reversal is different.

For structures with disorder, the moment in zero field is somewhat smaller than in the ordered case and the magnetization reversal is smoother at least for the wider systems (Fig. 7(b)). We see that for smaller widths ($w = 2$ and 4), there is a slight reduction of the magnetization before the sudden reversal. At a larger widths ($w > 6$), the jump is not present and the magnetization gradually reverses, indicating that at each field step only some of the magnetic moments are flipping. In these cases, the coercive field is increased by the presence of disorder, indicating that disorder stabilizes the existing magnetic structure, and delays its reversal. Again, we see that the coercive field (B_c) is almost determined by the width alone (Fig. 7(d)), but in this case, the results no longer match the prediction of the Stoner-Wohlfarth model.

Fig. 8 shows the evolution of the magnetic structure during this gradual reversal of the magnetization. As the applied magnetic field is increased, the magnetization reverses first in the central part of the strip, whereas the surfaces pin the moments and retain the original magnetic orientation for significantly larger fields. This essentially corresponds to the formation of two longitudinal domain walls. In the electron microscopy experiments of Varón *et al.*,[24] a single longitudinal domain wall is seen sweeping through the samples. This difference is most likely due to symmetry; in the simulations, only the disorder breaks the symmetry between the two edges, whereas the experimental structures tend to be bent and branched, and are in an inhomogeneous environment created by the stray magnetic fields of the surrounding structures.

In the absence of disorder, no longitudinal domain wall forms, and the magnetization flips in the entire sample at a
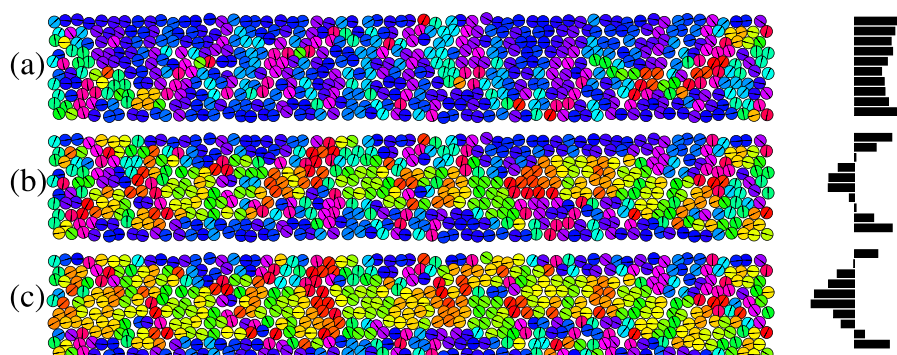

FIG. 8. Evolution of the magnetic order in disordered ferromagnetic systems with $l = 60$ and $w = 10$ in a reversed field of (a) 20 mT; (b) 40 mT; and (c) 50 mT. We see how the magnetization reverses in the central part of the system before it reverses at the long edges. The small plots show the magnetization projected along the long axis of the nanoparticle, as a function of lateral position, averaged over the length of the system. This confirms that the edges pin the moments.
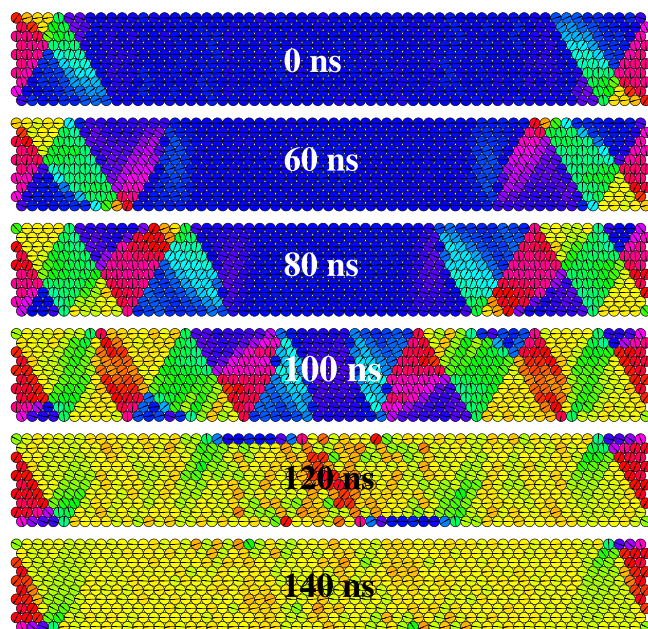
FIG. 9. Time-resolved reversal event in a fully ordered system ($w = 10$ and $l = 60$) when the reversing field is increased from 20 mT to 25 mT. Already after 60 ns, the moments are beginning to reverse near the two ends of the system, and after 120 ns, the system is fully reversed. The time scale depends on the moment of inertia of the particles and on the assumption that they rotate freely, and should not be taken as a prediction of the relaxation time of a real system.

critical field value. Fig. 9 shows the time evolution of such a flipping event in a system with $w = 10$ and $l = 60$. Since the simulations were made with the magnetic moment locked to the orientation of the particles, the time scale of this reversal is set by their moment of inertia. In the case of no magnetic anisotropy, the reversal of the moments would follow a similar path, but the magnetic dipoles would rotate without a corresponding rotation of the particles, and thus on a much shorter time scale.

It is seen in the ordered system (Fig. 9) that the field reversal is nucleated at the ends of the system, and propagates toward the central parts. As the reversing field is gradually increased, the magnetic structure initially remains in the F-state, but with a gradual increase in the relaxation structures at the two ends. These enhanced edge-effects at reversing fields up to 20 mT caused slight reduction of the magnetization before the abrupt reversal of the magnetization, as seen in Fig. 7(a). When the field is now switched on to the threshold field value 25 mT, the magnetic state is no longer stable and begins to flip. At 60 ns, the edge defects grew further into the structure and the field induced a flipping of the moments in a zig-zag-manner that continues until the entire system has reversed its magnetization at around 120 ns. The structure is an inverted relaxed F-state, indicating that the external field is competing with an oppositely pointing demagnetization field and the corresponding edge effects.

IV. CONCLUSIONS

We have simulated the energetics of domain walls in ferromagnetically coupled monodisperse assemblies of magnetic nanoparticles. As there is no exchange coupling between the nanoparticles, there is no associated exchange energy cost to domain wall formation, and the energetics of the domain walls are entirely controlled by the dipolar magnetic interactions between the nanoparticles. This makes it energetically favorable to form domain walls in the longitudinal direction of elongated nanoparticle assemblies instead of in the transversal directions, although assemblies with sufficiently high aspect ratio favor the fully ferromagnetic state. Introducing disorder in the arrangement of the nanoparticles does not significantly change this picture, but it does pin the magnetic domains and makes it harder to change the magnetization by an external applied field. In particular, longitudinal domain walls may be introduced into a ferromagnetically ordered assembly by a reverse applied field, but only if disorder is present.

[1]S. Bedanta, T. Eimüller, W. Kleemann, J. Rhensius, F. Stromberg, E. Amaladass, S. Cardoso, and P. P. Freitas, Phys. Rev. Lett. **98**, 176601 (2007).
[2]B. D. Terris and T. Thomson, J. Phys. D: Appl. Phys. **38**, R199 (2005).
[3]H. Zeng, J. Li, J. P. Liu, Z. L. Wang, and S. Sun, Nature **420**, 395 (2002).
[4]N. Jones, Nature **472**, 22 (2011).
[5]G. Hadjipanayis and A. Gabay, IEEE Spectrum **48**, 36–41 (2011).
[6]M. Klokkenburg, R. Dullens, W. Kegel, B. Erné, and A. Philipse, Phys. Rev. Lett. **96**, 037203 (2006).
[7]K. Butter, P. H. H. Bomans, P. M. Frederik, G. J. Vroege, and A. P. Philipse, Nature Mater. **2**, 88 (2003).
[8]J. R. Thomas, J. Appl. Phys. **37**, 2914 (1966).
[9]Z. Nie, A. Petukhova, and E. Kumacheva, Nat. Nanotechnol. **5**, 15 (2010).
[10]J. Henzie, J. E. Barton, C. L. Stender, and T. W. Odom, Acc. Chem. Res. **39**, 249 (2006).
[11]J. Zhang, Y. Li, X. Zhang, and B. Yang, Adv. Mater. **22**, 4249 (2010).
[12]S. Sun, S. Anders, H. F. Hamann, J. U. Thiele, J. E. E. Baglin, T. Thomson, E. E. Fullerton, C. B. Murray, and B. D. Terris, J. Am. Chem. Soc. **124**, 2884 (2002).
[13]E. Rabani, D. R. Reichman, P. L. Geissler, and L. E. Brus, Nature **426**, 271 (2003).
[14]J. M. Luttinger and L. Tisza, Phys. Rev. **70**, 954 (1946).
[15]M. Scheinfein, K. Schmidt, K. Heim, and G. Hembree, Phys. Rev. Lett. **76**, 1541 (1996).
[16]A. Sugawara and M. Scheinfein, Phys. Rev. B **56**, R8499 (1997).
[17]C. Djurberg, P. Svedlindh, P. Nordblad, M. Hansen, F. Bødker, and S. Mørup, Phys. Rev. Lett. **79**, 5154 (1997).
[18]V. F. Puntes, P. Gorostiza, D. M. Aruguete, N. G. Bastus, and A. P. Alivisatos, Nature Mater. **3**, 263 (2004).
[19]J. Chen, A. Dong, J. Cai, X. Ye, Y. Kang, J. M. Kikkawa, and C. B. Murray, Nano Lett. **10**, 5103 (2010).
[20]E. Y. Vedmedenko, A. Ghazali, and J. C. S. Levy, Phys. Rev. B **59**, 3329 (1999).
[21]A. J. Bennett and J. M. Xu, Appl. Phys. Lett. **82**, 2503 (2003).
[22]E. Y. Vedmedenko, Phys. Status Solidi **244**, 1133 (2007).
[23]K. Yamamoto, S. A. Majetich, M. R. McCartney, M. Sachan, S. Yamamuro, and T. Hirayama, Appl. Phys. Lett. **93**, 082502 (2008).
[24]M. Varón, M. Beleggia, J. Jordanovic, J. Schiøtz, T. Kasama, V. F. Puntes, and C. Frandsen, "Longitudinal domain wall formation in elongated assemblies of ferromagnetic nanoparticles," (to be published).

[25]M. P. Allen and D. J. Tildesley, *Computer Simulation of Liquids* (Clarendon Press, Oxford, 1987).

[26]H. J. C. Berendsen, J. P. M. Postma, W. F. van Gunsteren, A. DiNola, and J. R. Haak, J. Chem. Phys. **81**, 3684 (1984).

[27]J.-J. Weis, J. Phys.: Condens. Matter **15**, S1471 (2003).

[28]G. Held, G. Grinstein, H. Doyle, S. Sun, and C. Murray, Phys. Rev. B **64**, 012408 (2001).

[29]A. F. Gross, M. R. Diehl, K. C. Beverly, E. K. Richman, and S. H. Tolbert, J. Phys. Chem. B **107**, 5475 (2003).

[30]M. Varón, M. Beleggia, T. Kasama, R. J. Harrison, R. E. Dunin-Borkowski, V. F. Puntes, and C. Frandsen, Sci. Rep. **3**, 1234 (2013).

[31]A. Hubert and R. Schäfer, *Magnetic Domains: The Analysis of Magnetic Microstructures* (Springer, Berlin Heidelberg, 1998), p. 441.

[32]E. C. Stoner and E. P. Wohlfarth, Philos. Trans. R. Soc., A **240**, 599 (1948).